International Journal of Engineering and Advanced Technology (IJEAT)
ISSN: 2249-8958 (Online), Volume-7 Issue-2, December 2017

The Influence of Natural Gas Velocity on Hot Tapping Process

Eed A. Abdel-Hadi, Sherif H. T., Ahmed S. K., A. A. Al-Shafai

Abstract: ***The paper presents a numerical modeling of an arc welding as a heat source for the in-service natural gas pipeline at operating pressure 45 bar and 2 m/s velocity to allow predict peak temperature and cooling rate at specific points. Taking in to consideration all boundary conditions of fluid properties, ambient condition, and material specifications to achieve a sufficient model for the influence of natural gas velocity on the welding process to prevent the risk of hydrogen induced crack and burn through risk. Experiments were carried out on the national natural gas transmission pipeline in Egypt, during a hot tapping process for new branch execution, measurements and boundary conditions were recorded and then compared with numerical modeling analysis, furthermore, changing of natural gas velocity from 2 m/s to 20 m/s in numerical modeling were carried out to predict the risk of hydrogen induced crack and burn through; and to precise the safe range of gas velocity during hot tapping process.***

Keywords: hot-tapping process, velocity influence in-service welding, natural gas

I. INTRODUCTION

This paper describes and investigates the influence of natural gas velocity on hot tapping process by applying accurate field experiments to conduct and attach 6-inch carbon steel branch saddle on 32-inch carbon steel pipe with in-service filet welding, also 3D (three-dimensional) numerical model was adopted to simulate the welding process and the results of the numerical model are compared with those obtained from the experimental work.

A. Hot Tapping Process

Hot tapping is an alternative procedure that makes a new pipeline connection while the pipeline remains in service, with natural gas flowing inside under pressure. The hot tap procedure involves attaching a branch connection by welding it using any welding technique on the in-service main pipeline (operating pipeline) and installing a valve on the new branch, and then cutting out the operating pipeline wall within the branch and removing the wall section through the valve.

Manuscript published on 30 December 2017.
***** Correspondence Author (s)
Prof. Dr. Eed A. Abdel-Hadi*, Mechanical Engineering, Shobra Faculty of Engineering, Benha University, Cairo, Egypt, E-mail: eed.hafaz@yahoo.com
Prof. Dr. Sherif Hady Taher, Mechanical Engineering, Shobra Faculty of Engineering, Benha University, Cairo, Egypt, E-mail: sheriff.taher@feng.bu.edu.eg
Dr. Ahmed Mohamed Salah El-Said Kandil, Mechanical Engineering, Shobra Faculty of Engineering, Benha University, Cairo, Egypt, E-mail: agtc2001@yahoo.com
Eng. Ahmed Atef Al Shafai, Mechanical Engineering, Shobra Faculty of Engineering, Benha University, Cairo, Egypt, E-mail: eng.ahmedalshafai@gmail.com

Hot tapping avoids product loss, methane emissions, and disruption of service to customers but that from the economical point of view what about the other views of safety and lifetime for welding area. First, it is important to understand that hot tapping as an operation consists of two processes first process is welding the pipe sleeve or fitting which will be used for new branch, second process is the tapping or cutting the main pipeline wall (operating pipeline).

B. In Service Welding Gas Pipeline Problems

There are two significant problems when welding onto in-service pipelines. The first problem, the flowing gas creates a large heat loss through the pipe-wall due to convection heat transfer, resulting in acceleration of cooling rate for the weld. The influence of weld cooling rates causes a great hardness levels within the welding zone and in the heat affected zone (HAZ). As a result of increasing the hardness of the microstructure in the HAZ, there is an increased possibility of hydrogen induced cracking (HIC) due to the coarse grains of microstructure formation. The conditions needed for hydrogen-assisted cracking include hydrogen present to a sufficient degree, tensile stresses acting on the weld, and a susceptible**,** hard, HAZ microstructure [1-2-3].

The second problem concerns with the localized heating and loss of material strength during the welding process, since the pipe-wall may burst under internal pressure if this reduction in strength is too great. Pressurized natural gas (up to 45 bars) imposes a significant stress on the pipe wall, and since the strength of the pipe is decreased due to the localized heating during welding this can result in the failure of the pipe wall. The result can vary from a small localized bulging of the pipe wall, up to the bursting of the pipe. This is termed ‘burn-through’ and occurs when the region around the weld pool has insufficient strength to withstand the internal gas pressure.

C. Factors Influence Hot Tapping Process

The relevant factors which cover possibilities of heat affected zone (HAZ) crack or Hydrogen Induced crack (HIC) and factors influence burn through risk are as follows [4]: Heat Input, Welding Technique, preheat temperature, Welding Direction, fluid internal pressure, fluid temperature, fluid velocity, the thickness of base metal, base metal material and pipe diameter.

II. FIELD EXPERIMENT

Reinforced sleeve (branch saddle) with a total diameter of 6-inch and thickness of 7.1 mm was conducted to the main natural gas pipeline with outside diameter 32 inch and wall thickness of 12.7 mm during in service, a schematic illustration of sleeve welding onto the main pipe complete with fillet welding sequences is illustrated in Fig. (4),

The chemical composition and mechanical properties are shown in Table I and II respectively for pipe material.

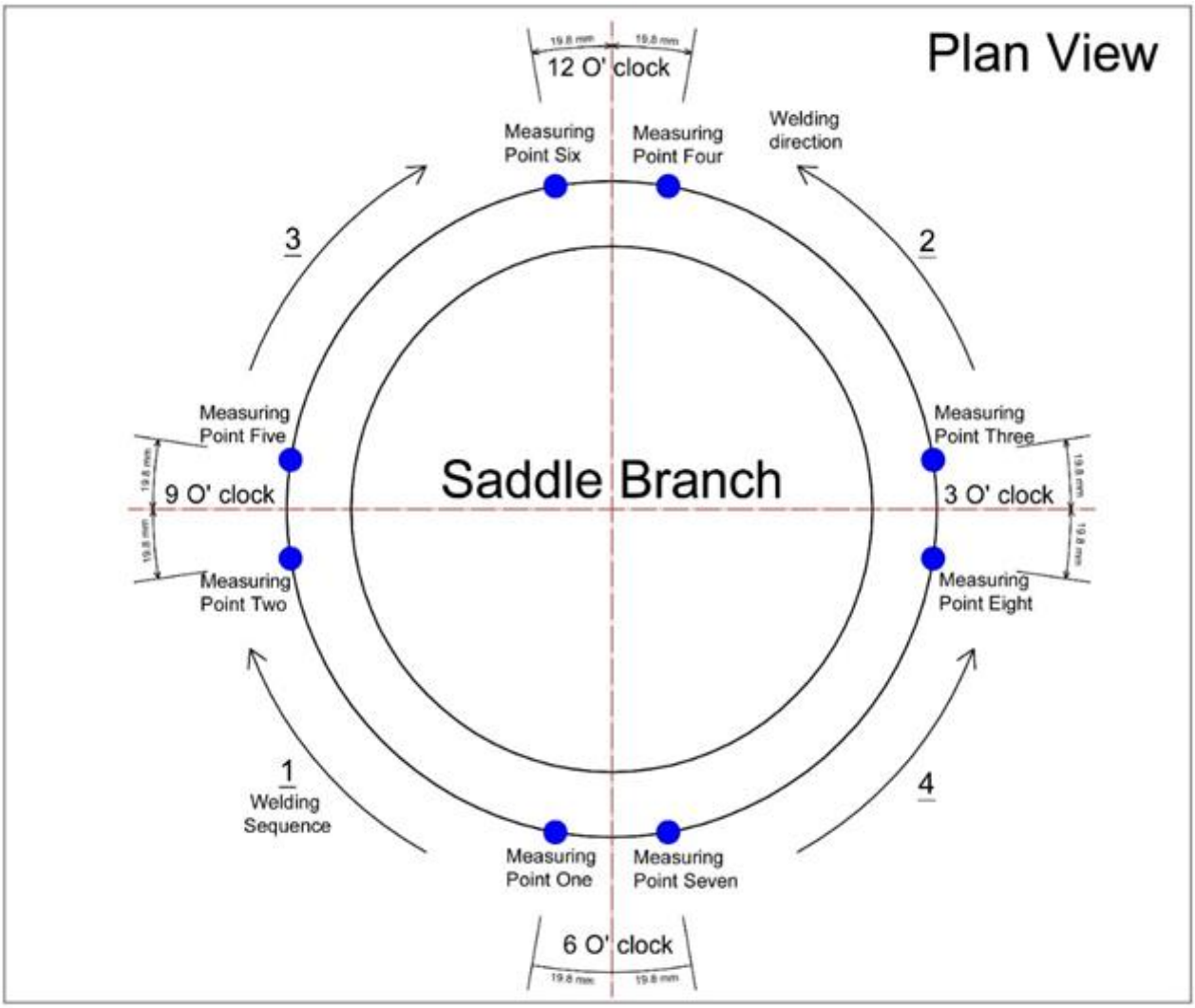

Fig.1. Welding Sequences and Experimental Measuring Point Arrangement

Table I Chemical Composition for Pipe and Branch Saddle

Chemical composition (wt - %)	
Pipe material	API 5L X52*
C – carbon	0.16
Si – silicon	0.45
Mn - manganese	1.6
Cu – copper	0.3
Ni – nickel	0.3
Cr – chrome	0.25
Mo – molybdenum	0.08
B – boron	0.0005
N – nitrogen	0.014
S – sulfur	0.001
P – phosphates	0.025
V – vanadium	0.06
Nb – niobium	0.05
Ti – thallium	0.04
Sn – tin	0.02

Table II Mechanical Properties for Pipe and Branch Saddle

Mechanical Properties	
Pipe material	API 5L X52
Yield strength (Min.)	52000 psi
Yield strength (Max.)	77000 psi
Tensile strength (Min.)	66000 psi
Tensile strength (Max.)	110000 psi
Elongation %	21

*API – American Petroleum institute standard for pipeline and steel grade is X52 represent min. yield strength.

The welding electrode used in welding process for first path is E 7018, which is a type of low hydrogen electrode with diameter of 3.2 mm, chemical composition and mechanical properties of deposited metal are listed in Tables III and IV respectively, for reduce the risk of HIC this type of electrodes required to be heated to 350 ˚C before beginning of welding process, for next welding paths, welding electrode type E 6010 was used for next filling three welding paths.

Published By:
Blue Eyes Intelligence Engineering and Sciences Publication (BEIESP)

Table III Chemical Composition Welding Electrode

Chemical Composition (wt - %)							
Pipe material	C	Si	Mn	Ni	S	P	V
E 7018	0.067	0.5	1.3	1.2	0.001	0.008	0.012

Table IV Mechanical Properties for Deposited Welding Metal

Mechanical Properties			
Pipe material	Yield strength Min.	Tensile strength Min.	Elongation %
E 7018	69069 psi	85260 psi	28

Average welding speed was 0.484 mm/s, welding parameters for shield metal arc welding (SMAW) technique were recorded and shown in Table IV, welding sequences was started with the first path from 6 to 9 O'clock (as indicated Fig. 2.), then second bead welded from 3 to 12 O'clock then third bead welded from 9 to 12 O'clock and lastly fourth bead welded from 6 to 3 O'clock every single quarter has a length of 132.18 mm and a total circumference of sleeve equal to 528.72, about 64 seconds was needed in order to accomplish first path welding per quarter. This welding sequence is used in order to reduce the heat input effect on the main pipe during welding in order to avoid excess heat input and risk of burn through possibility; Table V shows welding sequences.

Table V Welding Sequences

No.	Time of welding process (second)	Welding quarter	
		from	to
1	64	6 O'clock	9 O'clock
2	65	3 O'clock	12 O'clock
3	63	9 O'clock	12 O'clock
4	64	6 O'clock	3 O'clock

Figure (2) shows the configuration of the 6-inch branch on pressurized in service 32-inch pipeline. The internal pressure of 45 bars of natural gas was applied. The diameter and the thickness of the pipe are 32-inch and 12.8 mm respectively. The chemical composition of the pipe API 5L X52 pipe properties are shown in Table I, the saddle was also API 5L X52.

Fig. 2. Welding Sequences During Experiment in Field

A. Experimental Measurements

In order to accomplish high accuracy in measurements during the in-service welding process, measuring points were marked on the welding paths of branch saddle, these points are chosen from the center line of branch saddle as a datum line, two points per quarter welding path were used, one in start of path and the second point in the end of welding path with a fixed distance of 19.8 mm from diatom lines as shown in fig. (1).

Every measuring point was monitoring by using of inferred thermometer device which allowed to take and record about 99 temperature readings for the required measuring points.

These temperatures will be used to determine the cooling rate for cooling rate T8/5 and also will be used to determine the percentage of agreement between experimental work and 3D numerical model.

This measuring technique was used to measure and record temperature field for the eight measuring points on welding path during the in-service welding process, and allowed us to determine and figure out the cooling rate of welding, maximum surface temperature and also temperature distribution on HAZ.

After end of experiment, the temperature distributions of 8 testing points are obtained and also the change of temperature with time (cooling rate), which used to verify cooling rate from 800 ˚C to 500 ˚C – T8/5 – this time for temperature change is used to determine the hardness of welding deposit metal which predicted possibilities of hydrogen induced crack.

B. Numerical Modeling of the MSMAW Process

In shielded metal arc welding, a considerable amount of filler material is added continuously with the moving heat source. The energy added to the weld with this melted material accounts for a large part of the total energy. If the weld filler is assumed to be deposited with a certain initial temperature,

Published By:
Blue Eyes Intelligence Engineering
and Sciences Publication (BEIESP)

T1, e.g. of 1200°C, the energy released when the filler material is cooled to room temperature, T2, to this comes the release of latent heat is calculated from equation (1) [5]. These contributions are subtracted from the total power input equation (1), i.e.

$$Q_{filler} = Q_{total} - Q_{1-2} - Q_L = \eta UI - V\int_{T_1}^{T_2} \rho\, C_p\, dT - mL \quad (1)$$

Where $Q_{1\text{-}2}$, heat added for metal form ambient temperature (1) to maximum temperature (2), Q_L, latent heat, η, arc efficiency, U, volt, I, Current, V, volume of the filler material, m mass of the filler material, ρ, density and C, Specific heat.

In order to simulat the heat source distribution, the Gaussian surface heat source (fig. 3.) was used, which determine the heat flux for any point, Q (W/m^3) for a point within the spherical volume defined by the heat source.

The Gaussian surface heat source as indicated in fig.3. the heat flux at a point (x,y,z) within the circle of the welding arc center by the following equation[6]:

$$Q(x.y.z.t) = \frac{3*v*A*\eta}{\pi*r_0^2} * e^{-3\left[\frac{(x-x_0)^2+(y-y_0)^2+(z-z_0)^2}{r_0^2}\right]} \quad (2)$$

$$x_0 = v_x*t,\ y_0 = v_y*t,\ z_0 = v_z*t \quad (3)$$

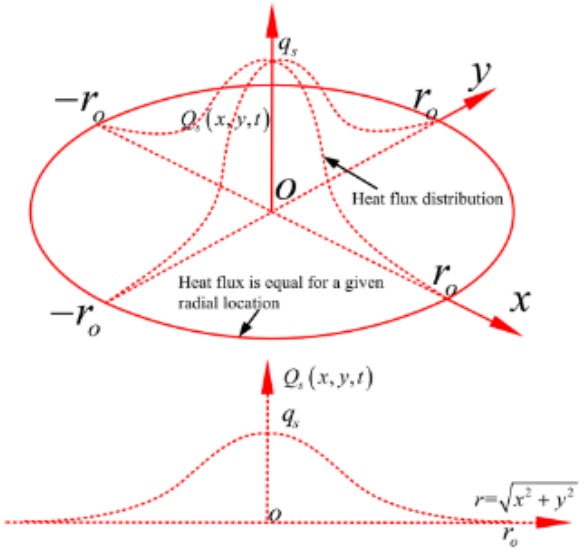

Fig. 3. Schematic Representation of a Gaussian Source and heat Flux Distribution

Where η is the arc efficiency for SMAW, V and I are voltage and current values, r_0 represents the Gaussian base radius, x, y, z are coordinate points to locate and define the motion of the welding torch along the weld path. The coordinate point x_0, y_0, z_0 is given by v*t, where v is the velocity of the welding torch and t is the welding time [7-8-9-10-11].

Various heat input was run in numerical model in order to accomplish a good understanding of flow velocity and it is the effect on cooling rate, heat inputs depending on the change of welding Ampere value was as shown in Table VI:

Table VI. Welding Heat Input

No.	Voltage, V	Ampere, A	Heat Input, Q W/m3
1	220	80	$4.9239*10^{12}$
2	220	85	$5.2316*10^{12}$
3	220	90	$5.5393*10^{12}$
4	220	95	$5.8471*10^{12}$
5	220	100	$6.1548*10^{12}$
6	220	105	$6.4626*10^{12}$

C. The moving heat source principle in the finite element model

The moving heat source methodology is applied in a three-dimensional finite element model in COMSOL. In order to simulate the welding process required to attach branch saddle with the main pipe a new technique is used by split the welding arc to short length straight line and by changing in coordinates and time, heat source which is moving along welding path using the equation (3) and step function without any smoothing tools to set starting and ending of heat source.

D. Numerical modeling of the heat transfer

During the welding process, the thermal field is governed by the heat conduction equation (4) which is given by:

$$\frac{\partial}{\partial x}\left(k(T)\frac{\partial T}{\partial x}\right) + \frac{\partial}{\partial y}\left(k(T)\frac{\partial T}{\partial y}\right) + \frac{\partial}{\partial z}\left(k(T)\frac{\partial T}{\partial z}\right) = \rho(T)C(T)\frac{\partial T}{\partial t} \quad (4)$$

Where; T, temperature, k(T), thermal conductivity, ρ(T) density and C (T), specific heat.

The thermal conditions on the external surfaces of the pipe include heat transfer for convection and radiation**.** The convection heat flow for (q_c) in gas or liquid environment is given by Newton's heat transfer law [4]**:** and given by equation (5):

$$q_c = h_c.(T-T_0) \quad (5)$$

Where; T is the temperature of the external surface, T_0 is the temperature of gas and h_c, convection heat transfer coefficient which depends on the convection conditions on the solid surface, also the surface properties and the environment.

The heat flow rate by radiation, q_r is governed by the Stefan-Boltzmann law, as follows [12] and given by equation (6)**:**

$$q_r = \varepsilon_r.\ \sigma_r.(T^4-T_0^4) \quad (6)$$

Where; ε emissivity of the material surface and σ_r is the Stefan-Boltzmann constant.

E. Meshing of Numerical Model

1. Branch Saddle

Triangular mesh type as given in fig. 4. was used for meshing process to branch saddle with two size for elements first one is extremely fine mesh with maximum element size 0.015 m that for entire surfaces of branch saddle except for surfaces contact to welding process maximum element size used was 0.0012 m in order to get more accurate temperature profile and study of cooling rates.

Published By:
Blue Eyes Intelligence Engineering
and Sciences Publication (BEIESP)

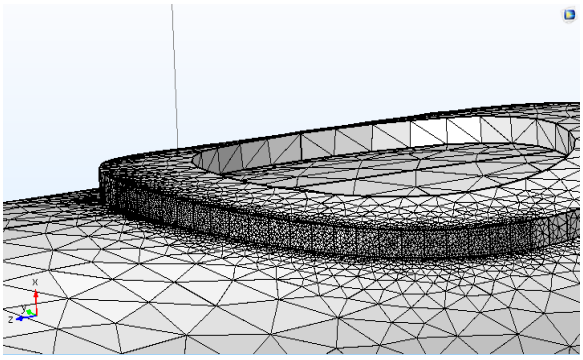

Fig. 4. Geometry Meshing of Numerical Model

2. Pipes and fluid:

Triangular mesh type as given in Fig. 4 was used for meshing process to pipes and fluid size of mesh with maximum element size of 0.0656 m.

F. Hardness Calculations

In order to determine the possibilities of cold crack it is required to check the hardness of heat affected zone after in-service welding process, due to the high cooling rate of natural gas, the possibilities of Hydrogen induced crack is depended on cooling rate of welding zone.

Assessment of cold cracking for the maximum HAZ hardness is often limited to 350 HV in welding fabrication of offshore structures and pipe lines for avoiding risk of cold crack, the previous study showed HAZ micro-structures with a hardness of 248 HV and higher are susceptible to stress crack after completion of in-service welding used to transport mildly sour gas (which includes h_2S contains).

Formulas that estimating maximum HAZ hardness from various carbon equivalents in conjunction with welding parameters, such as cooling time and reduction for welding zone temperature from 800 ˚C to 500 ˚C, T8/5, Yurika formula (1981) [13,14] has the widest applicable range among the formulae which is given by the followings equations:

$$t_m = 10^{\left(\frac{611.3C+605.7C_{eq}-239}{1009.5C+52.8}\right)} \quad (7)$$

$$t_b = 10^{\left(\frac{1413.3C+300.7C_{eq}-35}{1009.5C+52.8}\right)} \quad (8)$$

For T8/5 ≤ tm

$$HV_m = \frac{1}{2}\left\{802C + 305 + 406C + 164CE_I + 183 - (369C - 149CE_I + 100)\tan^{-1}\left(\frac{\log_{10} t_m - 2.822CE_{II} + 0.262}{0.526 - 0.195CE_{II}}\right)\right\} \quad (9)$$

For T8/5 ≥ tb

$$HV = \frac{1}{2}\left\{305C_{eq} + 101 + 406C + 164CE_I + 183 - (369C - 149CE_I + 100)\tan^{-1}\left(\frac{\log_{10} t_{8/5} - 2.822CE_{II} + 0.262}{0.526 - 0.195CE_{II}}\right)\right\} \quad (10)$$

For tm ≤ T8/5 ≤ tb

$$HV = \frac{1}{2}\left\{2019\left[C\langle 1 - 0.5\log_{10} t_{8/5}\rangle + 0.3(C_{eq} - C)\right] + 66(1 - 0.8\log_{10} t_{8/5})\right\} + \frac{1}{2}\left\{406C + 164CE_I + 183 - (369C - 149CE_I + 100)\tan^{-1}\left(\frac{\log_{10} t_{8/5} - 2.822CE_{II} + 0.262}{0.526 - 0.195CE_{II}}\right)\right\} \quad (11)$$

Where C is the Carbon content in wt%

$$C_{eq} = C + \frac{Si}{11} + \frac{Mn}{8} + \frac{Cu}{9} + \frac{Ni}{17} + \frac{Cr}{5} + \frac{Mo}{6} + \frac{V}{3} \quad (12)$$

$$CE_I = C + \frac{Si}{24} + \frac{Mn}{6} + \frac{Cu}{15} + \frac{Ni}{40} + \frac{Cr}{6} + \frac{Mo}{4} + \frac{V}{5} + \frac{Nb}{5} + 10B \quad (13)$$

$$CE_{II} = C + \frac{Si}{30} + \frac{Mn}{5} + \frac{Cu}{5} + \frac{Ni}{20} + \frac{Cr}{4} + \frac{Mo}{6} + 10B \quad (14)$$

Where t_m, cooling time giving 100% martensite, t_b cooling time giving 100% bainite, C_{eq}, carbon equivalent for metal, HV, hardness Vickers.

Equations above were used to predict maximum HAZ hardness from pipe chemical composition, measured cooling rate from experimental work and calculated cooling time from the thermal analysis obtained from numerical modelling, the occurrence of cold cracking was assessed by comparison between the calculated maximum HAZ hardness and the limited hardness 350 HV, this algorithm gives the predication hardness with standard deviation of 28 HV, Table VII shows that those from HAZ hardness calculations for eight measuring points and numerical model results also depend on $T_{8/5}$.

III. RESULTS AND DISCUSSION

In order to investigate the effect of natural gas velocity on hot tapping process, $T_{8/5}$ cooling temperature had determined for 8 measuring points during in-service fillet weld for branch saddle as illustrate in fig. 2. using accurate inferred thermometer, cooling rate and temperature distribution results of 8 measuring points are illustrating in the next figures.

A. Experimental Results

the peak temperature for first measuring point on welding path 6-9 O'clock during in-service welding is 1078 ˚C as shown in fig. 5., also the T8/5 about 9.5 seconds to reduce welding temperature from 800 ˚C to 500 ˚C starts from second 13 to second 22.5. for second measuring point on welding path 6-9 O'clock the peak temperature during in-service welding is 1095 ˚C is shown in fig. 6., also the T8/5 was about 8.5 seconds to reduce welding temperature from 800 ˚C to 500 ˚C starts from second 63.3 to second 73.5.

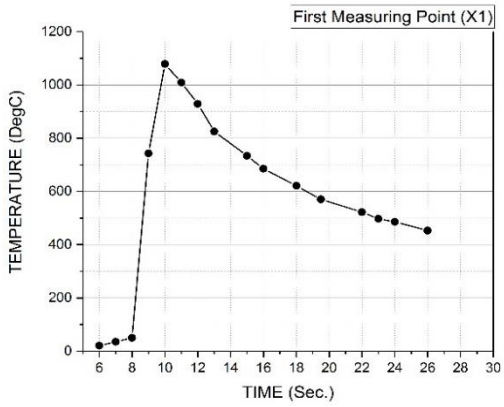

Fig. 5. First Measuring Point (X1)

Published By:
Blue Eyes Intelligence Engineering
and Sciences Publication (BEIESP)

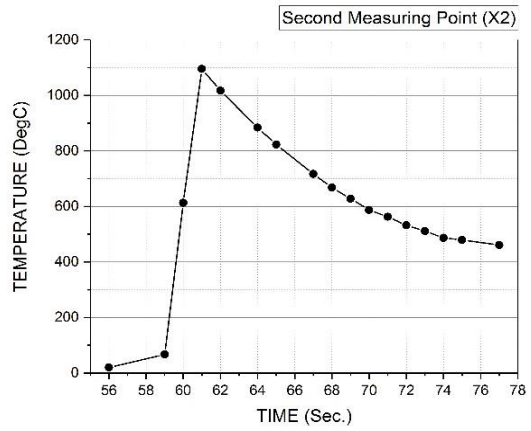

Fig. 6. Second Measuring Point (X2)

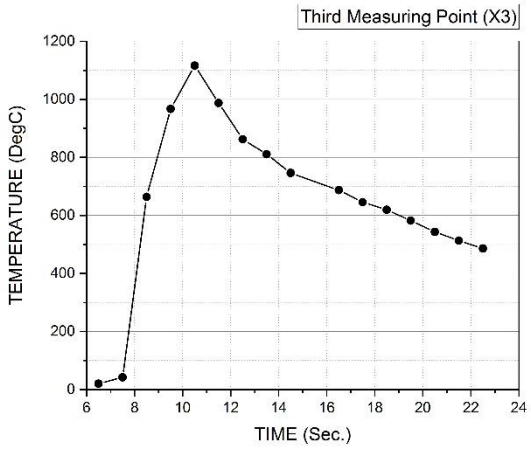

Fig. 7. Third Measuring Point (X3)

The third measuring point on welding path 3-12 O'clock during in-service welding record peak temperature for is 1116 ˚C as shown in fig. 7., also the T8/5 was about 8.2 seconds to reduce welding temperature from 800 ˚C to 500 ˚C starts from second 16.3 to second 24.5.

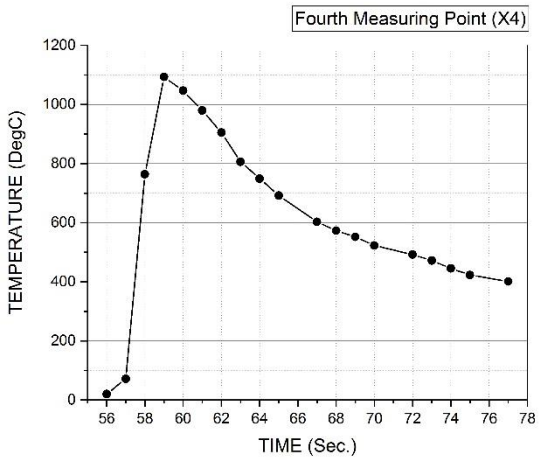

Fig. 8. Fourth Measuring Point (X4)

The peak temperature for fourth measuring point on welding path 3-12 O'clock during in-service welding is 1093 ˚C as shown in fig. 8., also the T8/5 was about 8.1 seconds to reduce welding temperature from 800 ˚C to 500 ˚C starts from second 63.1 to second 71.1. The peak temperature for fifth measuring point X5 on welding path 9-12 O'clock during in-service welding is 1018 ˚C as shown in fig. 9., also the T8/5 was about 8 seconds to reduce welding temperature from 800 ˚C to 500 ˚C starts from second 13.1 to second 21.1.

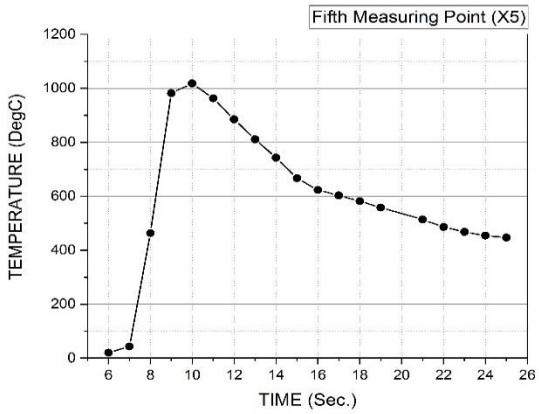

Fig. 9. Fifth Measuring Point (X5)

and the peak temperature for Sixth measuring X6 point on welding path 9-12 O'clock during in-service welding is 1051 ˚C as shown in fig. 10., also the T8/5 was about 8.7 seconds to reduce welding temperature from 800 ˚C to 500 ˚C starts from second 65.5 to second 74.2

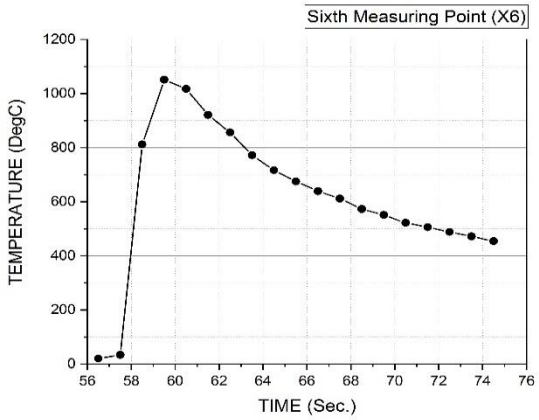

Fig. 10. Sixth Measuring Point (X6)

The peak temperature for seventh measuring point X7 on welding path 6-3 O'clock during in-service welding is 1068 ˚C as shown in fig. 11., also the T8/5 was about 7.4 seconds to reduce welding temperature from 800 ˚C to 500 ˚C starts from second 16.5 to second 23.9.

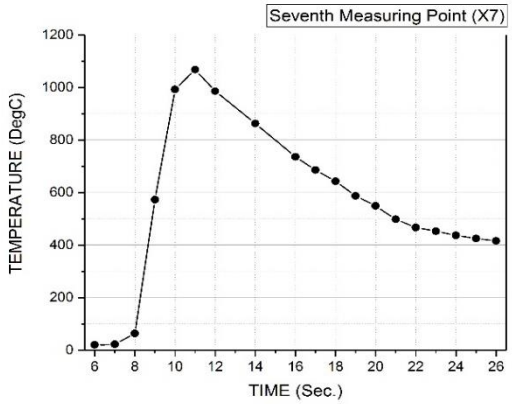

Fig. 11. Seventh Measuring Point (X7)

Published By:
Blue Eyes Intelligence Engineering and Sciences Publication (BEIESP)

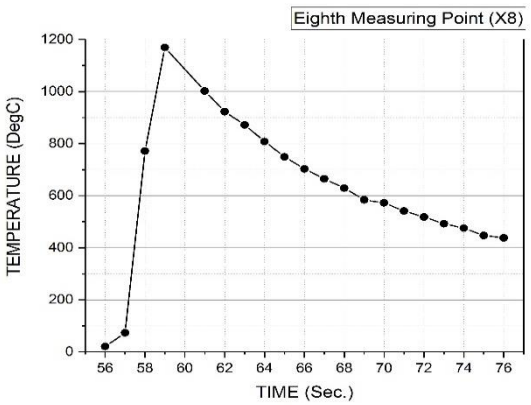

Fig. 12. Eighth Measuring Point (X8)

The peak temperature for eighth measuring point X8 on welding path 6-3 O'clock during in-service welding is 1169 ˚C as shown in fig. 12., also the T8/5 was about 8 seconds to reduce welding temperature from 800 ˚C to 500 ˚C starts from second 69.1 to second 77.1.

B. Numerical Results

Sequences of models using the 3D-time-depend-analysis were solved using same parameters defined in the field welding (experimental work) which describes pipe geometry and flow conditions, the numerical models were used to calculate T8/5 cooling time and maximum temperature in inner surface for pipe under welding pool during in-service welding. The 3D transient fillet in-service weld results are compared with field fillet weld results to determine deviation.

Figure 13 shows 3D numerical results for one measuring points on welding path 6-9 O'clock as shown in fig. 1.

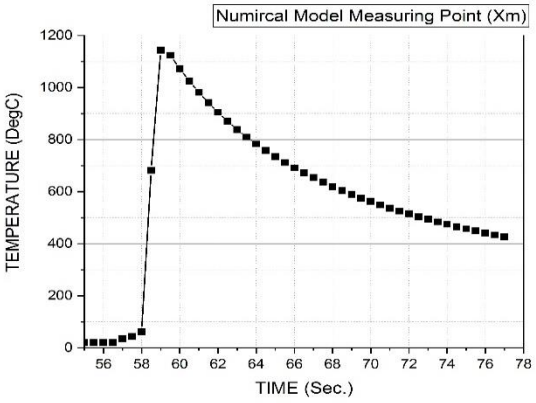

Fig. 13. Numerical Model Results

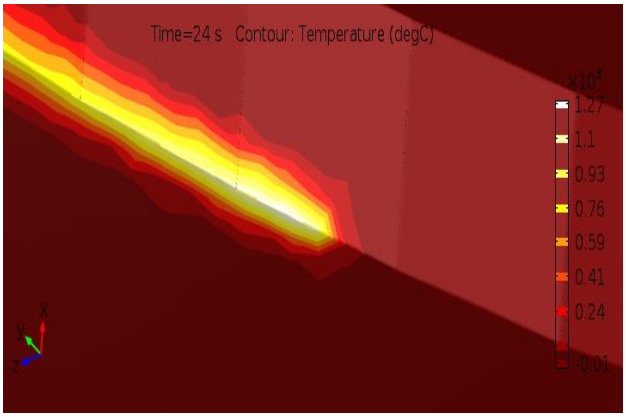

Fig. 14. Temperature Contours

Figure 14 illustrates the temperature contours during in-service welding for welding path 6 – 9 O'clock, with total welding time t=64 (s) inner service temperature was 46 ˚C in the main pipe and maximum temperature in welding pool (fusion zone) is 1116 ˚C.

C. HAZ Hardness Results

Hardness of HAZ in welding zone was calculated depending on measuring of T8/5 from both experimental work and numerical model and illustreated in equations from (7-14).

Table VII Hardness Calculations for Welding Zone

Hardness Results for Experimental Work		
Measuring point	T8/5 (s)	HAZ Hardness
X1	9.5	409.1693423 ±28 HV
X2	8.5	416.0635574 ±28 HV
X3	8.2	418.2502325 ±28 HV
X4	8.1	418.9927027 ±28 HV
X5	8	419.7422543 ±28 HV
X6	8.7	414.638076 ±28 HV
X7	7.4	424.3991698 ±28 HV
X8	8	419.7422543 ±28 HV
Hardness results for numerical model		
Xn	8.39	413.0150 ±28 HV

IV. CONCLUSIONS

From the above analysis and discussion of the influences of natural gas velocity on hot tapping process presented in this paper it can be concluded the following:

1. Good completion and agreement between experimental measurements and numerical model results were efficiently achieved, this shows that the numerical model can be used to expect both the risk of burn through and HIC.
2. Risk of burn through was not expected at all due to that the inner surface temperature of pipe does not increase more than 122 ˚C, according to several runs for heat input in the numerical model and different natural gas velocity.
3. Several velocities for natural gas were used in the numerical model but changes in temperature of the inner surface or temperature distribution and cooling rate shows small effects due to the large diameter of the main pipe.
4. Risk of hydrogen induced crack (HIC) due to increasing of HAZ hardness was expected with 5% according to the result of experiment and T8/5 for V=220 volt, A=80, and $\eta = 0.8$. and according to numerical modelling it is required to increase the heat input for about volt = 220 V, current =100 -105 A.
5. The maximum HAZ hardness shows small changes with the increase in gas flow rate.

Published By:
Blue Eyes Intelligence Engineering
and Sciences Publication (BEIESP)

6. Influence of natural gas velocity has no effect on both HIC or burn through risk.
7. From the numerical simulation, it can be suggested that the sleeve-repair welding of API 5L X52 pipelines of 12.8 mm thickness can be carried out without burn through at the maximum operating pressure (45 bar). To avoided cold crack, it is suggested to increase the heat input.

REFERENCES

1. Cen K., Zhang D. and Yin J., Numerical Simulation of Sleeve Repair Welding on In-service 16Mn Crude Oil Pipelines.
2. Xiaolong X., Jia-Gui Z. and Widera G.E.O., 2007, Numerical Simulation of In-Service Welding of a Pressurized Pipeline, ASME Journal.
3. Zhu J., Xue X. and Sang Z., 2005, Study on Design Pressure of In-service Welding Pipes, Technological Sciences Journal.
4. M.J.Painter and P. Sabapathy, 2000, In-Service Welding of Gas Pipelines, The University of Adelaide.
5. Jan L. H.,2003. Numerical modeling of welding induced stresses, Technical University of Denmark.
6. Bang I. W., Son Y.-P., Oh K. H., Kim Y. P. and Kim W. S., 2002, Numerical Simulation of Sleeve Repair Welding of In-Service Gas Pipelines, Welding Journal
7. Farid V. T. and Hamed M., 2009, Two-Dimensional Thermomechanical Analysis of Burn-Through at In-Service Welding of Pressurized Canals, Journal of Applied Sciences.
8. Sabapathy P.N, Wahab M.A., Painter M.J., 2001, Numerical Models of In-Service Welding of Gas Pipelines, Journal of Materials Processing Technology.
9. Ying W., Lijun W., Xinjie D., Yeteng S., Xiuwei B., AND Xiumin G., 2013, Simulation and analysis of temperature field for in-service multi-pass welding of a sleeve fillet weld, Computational Materials Science.
10. Dr.Muna K. Abbass, Dr. Jalal M. Jalil, and Dr. Abbas Sh. Alwan, 2010, Numerical Simulation of In-Service Welding of a Pressurized Pipeline, Eng.&Tech. Journal, Vol.28, No 12.
11. Goldak, J., Chakravarti, A., and Bibby, M. 1984, A new finite element model for welding heat sources. Metall. Trans.
12. Holman J. P., 1992, Heat transfer, 7th edition, McGraw-Hill, New York.
13. Kasuya, T., Yurioka, N., and Okumura M., 1995, Methods for predicting maximum hardness of heat-affected zone and selecting necessary preheat temperature for steel welding. Nippon Steel Technical Report 65(4): 7–14.
14. Joanna M. N., 2008, The prediction of maximum HAZ hardness in C-Mn and low alloy steel arc welds, International Conference 'Computer Technology in Welding and Engineering, University of Cranfield.

Published By:
Blue Eyes Intelligence Engineering and Sciences Publication (BEIESP)